RF and Power Characteristics of AlGaN/AlN/GaN HEMTs on Mn-Doped Freestanding GaN substrate

Chien-Hsian Chao [1], Hsien-Chin Chiu[1], Hsiang-Chun Wang[1], Chong Rong Haung[1], Chen Kang Chuang[1], Yang Ching Ho[1]

[1] Department of Electronics Engineering, Chang Gung University, Taiwan, R.O.C.

TEL: +886-3-2118800 # 3645 Email: hcchiu@mail.cgu.edu.tw

Keywords: GaN on GaN, Mn dopant, Load-Pull, High Frequency

Abstract

This study investigates Mn/Fe-doped AlGaN/AlN/GaN high electron mobility transistors (HEMTs) grown on a GaN substrate. According to X-ray-diffraction profiles, the smaller full width at half-maximum value of the Fe-doped GaN HEMT compared to the Mn-doped GaN HEMT indicates that Fe-doped GaN HEMT has lower dislocation density. However, the Mn-doped device outperforms the Fe-doped device in the transmission line. Consequently, DC measurements show that the Fe dopant slightly outperforms the Mn dopant. However, high-frequency and load–pull measurements show the advantages of the Mn dopant owing to its smaller transmission line.

INTRODUCTION

High-electron-mobility transistors (HEMTs) are used in high-frequency and -power devices owing to their superior material properties, such as high-electron velocity, high breakdown field, and high operating temperature [1]. AlGaN/GaN heterostructures can be grown on sapphire, silicon, silicon carbide, and native GaN substrates. Silicon is a common substrate material owing to its low cost [2]. However, radio frequency (RF) performance is still limited by different electron-trapping effects, where DC–RF dispersion and the memory effect are partly caused by traps located in the buffer [3]. Furthermore, high lattice-mismatch density is a notable drawback of GaN on Si. This study utilizes GaN substrates with Mn/Fe doping to compare the advantages of each dopant. The Mn acceptor level is derived as 1.8 eV below the bottom of the GaN conduction band [9].

EXPERIMENTAL PROCEDURES

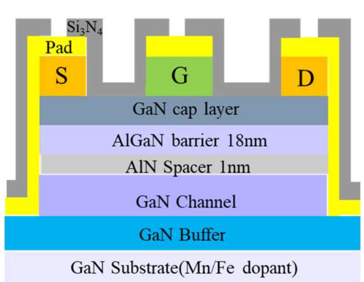

Fig.1 Cross sectional schematic of GaN HEMT.

In this study, a GaN/AlGaN/AlN//GaN/SiC/Si HEMT was grown on 6-inch GaN substrates by metal-organic chemical vapor deposition. The layer stack consists of a 300-nm GaN buffer layer, a 900-nm GaN channel layer, a 1-nm spike layer, an 18-nm AlGaN barrier layer, a 2-nm GaN cap, and a 4.5-nm Si_3N_4 cap, as depicted in Fig. 1(a).

The first fabrication process was mesa isolation using $Cl_2/BCl_3/Ar$ by reactive ion etching. Second, source/drain ohmic contacts were formed using Ti/Al/Ni/Au (25/130/25/90 nm) by e-beam evaporation and subsequently alloyed at 900°C for 30 s in ambient N_2. Next, the Ni/Au gate metal was defined, and Ti/Au was deposited as the pad. Finally, the device was passivated with Si_3N_4 by plasma-enhanced chemical vapor deposition.

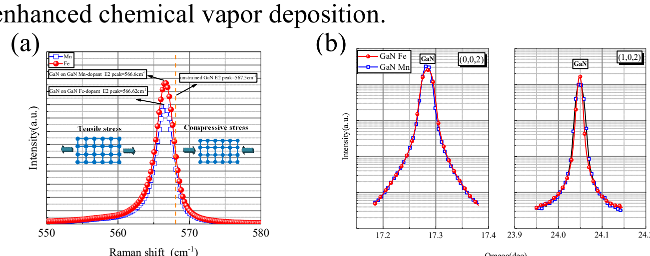

(c)

	FWHM(002) (arcsec)	FWHM(102) (arcsec)	Dislocation(crew) (cm^2)	Dislocation(edge) (cm^2)	Dislocation(total) (cm^2)
GaN Mn	59.76	54	7.16E+6	1.55E+7	2.266E+7
GaN Fe	75.24	32.76	1.14E+7	5.71E+6	1.711E+7

Fig. 2 (a) Raman diagram; (b) X-ray diffraction profiles of GaN HEMT structure on Mn/Fe-doped GaN substrates; (c) dislocation density of two devices.

RESULTS AND DISCUSSION

Fig.2(a) shows the Raman measurement results of the Mn/Fe-doped GaN HEMT. The principle of Raman measurement is to use a fixed wavelength of laser light to excite the sample. The photon-molecule collisions cause energy exchange, which changes the frequency of the light. This change is called the Raman shift. The Raman displacement of the pure GaN film without any stress is 567.6 cm^{-1}. Meanwhile, the Mn-doped GaN HEMT test piece has an offset of 566.62 cm^{-1} [4], the Fe-doped GaN HEMT test piece has an offset of 566.6 cm^{-1}, and the Raman displacement of the two test pieces. Because the peak value of the displacement is small, both test pieces are subjected to tensile stress. Furthermore, the Fe-doped GaN HEMT test piece has more deviations and bears greater tensile stress, which increases buffer layer defects, thereby affecting the reliability of its components. Fig.2 (b) shows the XRD measurement results of the Mn- and Fe-doped GaN HEMTs. The FWHM of the measurement results can be used to determine the degree of the misalignment between the GaN buffer layer and the substrate junction in the transistor [5]. The lower FWHM value of the Fe-doped GaN HEMT indicates less dislocation density. The dislocation densities of SiC on the Mn- and Fe-doped GaN HEMTs are approximately 2.266×10^7 and 1.711×10^7 cm^{-2}, respectively.

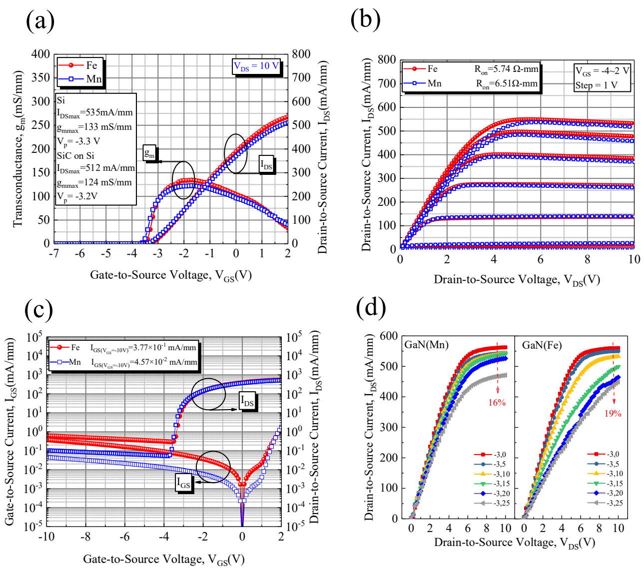

Fig. 3 (a) Measured I_{DS}–V_{GS} at V_{DS} = 10 V of devices; (b) Measured I_{DS}–V_{DS} at V_{GS} ranging from −4 to 2 V of devices; (c) Measured I_{DS}–V_{DS} and I_{GS}–V_{GS} characteristic diagram; (d) Measured pulse measurement characteristic diagram.

Fig.3(a) shows the I_{DS}–V_{GS} characteristics of the Mn- and Fe-doped GaN HEMTs. The gmmax values of the Mn- and Fe-doped GaN HEMTs are 124 and 133 mS/mm, respectively. Fig.3(b) shows the I_{DS}–V_{DS} characteristics of the Mn- and Fe-doped GaN HEMTs. The Ron values of the Mn- and Fe-doped GaN HEMTs are 6.51 and 5.74 Ω mm, respectively. The Fe-doped GaN HEMT has higher DC characteristics due to its lower dislocation density. The I_{DS}–V_{DS} and I_{GS}–V_{GS} characteristic diagrams of the Mn- and Fe-doped GaN HEMTs shown in Fig.3(c) can be used to analyze the characteristics of the Schottky gate. The measurement conditions are as follows: V_{DS} = 0 V, V_{GS} ranges from −10 to 2 V, V_{GS} = −10 V (off state), the gate leakage current I_{GS} of the Mn dopant element is 4.57×10^{-2} cm^{-2}, and the I_{GS} of the Fe dopant element is 3.77×10^{-1} cm^{-2}. Fig.3(d) shows the pulse-measurement characteristic diagrams of the HEMTs. The drain-lag measurement is performed using a pulse-measurement system, where the drain bias is applied to the device while it is in the off state and electrons are captured by the defects of the buffer layer due to the negative bias voltage of the gate and the high electric field, resulting in electrons being trapped when the device is turned on instantly. Defect capture produces a current-collapse effect [6]. In this experiment, the AM241 drain measurement module and the AMCAD pulse-measurement system are used to conduct the pulse measurement. The gate pulse width is 20 µs, the pulse period is 200 µs, the duty cycle is 10%, the gate static bias voltage VGSQ = −3 V, and the drain static bias voltage VDSQ = 0, 5, 10, 15, 20, and 25 V. The maximum current value of the two components began to decrease because of the current-collapse effect, the Mn-doped component decreased by 12.9%, whereas the Fe-doped component decreased by 19%. The large size of the Mn-doped element means that electrons are more severely trapped by defects because the greater tensile stress results in more defects in the buffer layer of the Fe-doped element.

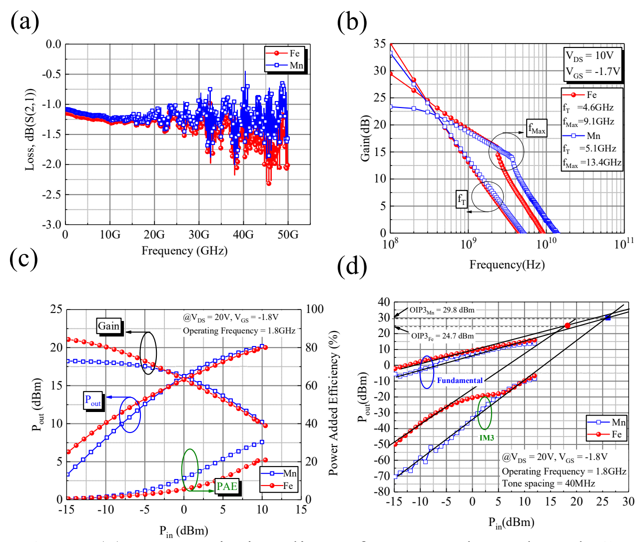

Fig. 4 (a) Transmission line of Mn- and Fe-doped GaN HEMTs; (b) high-frequency of Mn- and Fe-doped GaN HEMTs; (c) measured load–pull characteristic diagrams of Mn- and Fe-doped GaN HEMTs; (d) Measured two-tune measurement characteristic diagrams of Mn- and Fe-doped

Fig.4(a) illustrates that the Mn-doped GaN HEMT experienced greater substrate loss than the Fe-doped GaN HEMT. Fig.4(b) shows the high-frequency characteristics of the Mn- and Fe-doped GaN HEMTs. V_{DS} = 10 V, V_{GS} = −1.3 V, and the current-gain cutoff frequencies of the Mn- and Fe-doped GaN HEMTs are 5.1 and 4.6 GHz, respectively. The maximum frequencies of oscillation of the Mn- and Fe-doped GaN HEMTs are 13.4 and 9.1 GHz, respectively. The Mn-doped GaN HEMT has better high-frequency characteristics because of its lower substrate loss. Fig.4(c) shows the load–pull of the Mn- and Fe-doped GaN HEMTs. The power-added efficiency of the Mn- and Fe-doped GaN HEMTs is 29.85% and 21.89%, respectively. Fig.4(c) shows the two-tune of the Mn- and Fe-doped GaN HEMTs. The OIP_3 values of the Mn-and Fe-doped GaN HEMTs are 29.8 and 24.7 dBm, respectively.

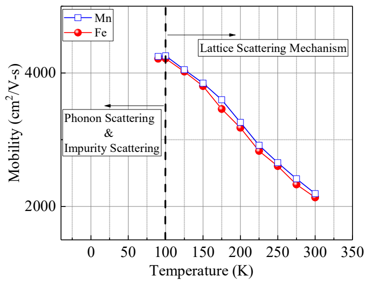

Fig. 5 Temperature-dependent Hall measurement of Mn- and Fe-doped GaN HEMTs

Fig.5 shows the temperature-dependent Hall measurements of the Mn- and Fe-doped GaN HEMTs. The relationship between the temperature and the electron mobility of the devices can determine the scattering mechanism of the epitaxial lattice; the general temperature-variable Hall measurement range is 20 K–300 K (R.T.), as the measurement temperature decreases from room temperature to 100 K. Previously, the influence of lattice and phonon scattering caused by the lattice vibration was decreasing, substantially increasing electron mobility. Phonon scattering includes optical phonon scattering and acoustic phonon scattering [7]. At room temperature 300 K, the electron mobility of Mn- and Fe-doped components are 2192 cm^2/V-s and 2135 cm^2/V-s, respectively, demonstrating that the electron mobility of the Mn-doped component is slightly higher than that of the Fe-doped component. The influence of lattice scattering decreases with the temperature, which increases electron mobility. At 100 K, the electron mobility of the two components reaches 4256 and 4216 cm^2/V-s, respectively. Further decrease in temperature leads to scattering in both components by impurities. Both components tend to decline, and there is a remarkable difference between them when the crystal lattice is scattered above 100 K.

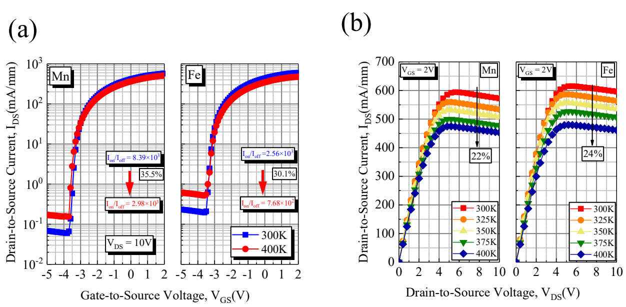

Fig. 6 (a) Measured temperature-dependent I_{DS}–V_{GS} at V_{DS} = 10 V of devices, (b) Measured temperature-dependent I_{DS}–V_{DS} at V_{GS} = 2 V of devices

Fig.6(a) shows the temperature-dependent I_{DS}–V_{GS} characteristics of the Mn- and Fe-doped GaN HEMTs. Use the heating chamber to raise the temperature of the element and conduct DC-flow measurements at room temperature (300 K) and a high temperature (400 K), respectively. The DC characteristics decrease as the temperature increases, and the on–off ratio (I_{on}/I_{off}) of the Mn-doped element decreases from 8.39×10^3 to 2.98×10^3, leaving 35.5%, whereas that of the Fe-doped element decreases from 2.56×10^3 to 7.68×10^2, leaving 30.1%. As the high-temperature Mn-doping resistance is higher than that of Fe doping [8], the leakage current increase lessens, resulting in a smaller proportion of current-switching ratio degradation. Fig.6(b) shows the temperature-dependent I_{DS}–V_{DS} at V_{GS} = 2 V of the Mn- and Fe-doped GaN HEMTs. The on-resistance increases with the temperature; the on-resistance (Ron) of the Mn- and Fe-doped components increase from 5.9 to 6.77 Ω-mm, and 5.32 to 6.88 Ω-mm, respectively; while the resistance values of both components increase by 115% and 125%, respectively. It can be inferred that the Mn-doped substrate has better thermal conductivity, which makes the transistor dissipate heat quickly; thus, the Mn-doped device has better reliability under variable-temperature conditions.

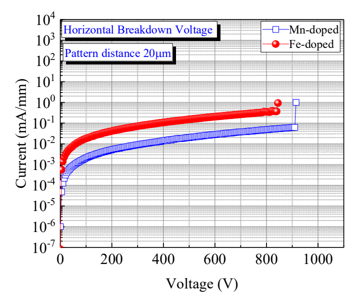

Fig. 7 Horizontal breakdown voltage measurements of Mn- and Fe-doped GaN HEMTs

Fig.7 shows the horizontal breakdown voltage measurements of the Mn- and Fe-doped GaN HEMTs. The distance between the two measurement endpoints is 20 µm. Because the buffer layer has been etched between these two endpoints, the purpose of the measurement is to analyze the GaN buffer layer on the two substrates. The Agilent B1505 can produce a voltage of up to 3000 V; a collapse is defined as the point when the current reaches 1 mA/mm. The breakdown voltages of Mn and Fe doping are 915 V and 830 V, respectively. The breakdown voltage of the Mn-doping element level is better, indicating that its buffer layer The epitaxial quality of Fe-doped is better than that of Fe-doped.

Fig.8 shows the thermal image measurements of the Mn and Fe-doped GaN HEMTs. Thermal images provide insights into changes in the surface temperature of the components during operation. The thermal imager can measure the distribution and temperature of the surface of the components. Place the components under the thermal imager for continuous monitoring and give them a bias voltage at 10 s. Operate them at a current of 60 mA for 300 s, and the elements will generate heat and heat up. The maximum temperatures of the Mn- and Fe-doped surfaces are 31.5°C and 31.8°C, respectively, and the Mn-doped temperature between the two rises is slower than that of Fe doping, and its heat dissipation is better than that of Fe doping.

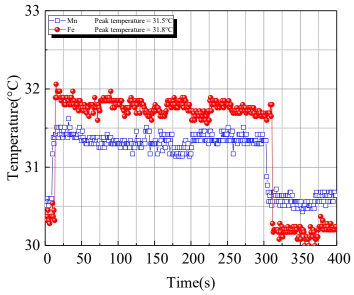

Fig. 8 Thermal image measurements of Mn- and Fe-doped GaN HEMTs

CONCLUSIONS

In this study, we compared two different substrate dopants with Mn and Fe. We demonstrated the advantages of Fe dopant in terms of DC characteristics due to its lower dislocation density. Furthermore, we demonstrated the advantages of Mn dopant in terms of RF performance due to its better substrate loss. As a result, we can experiment with new dopants such as Mn for use in high-frequency devices. GaN high-frequency structures are grown on Mn- and Fe-doped GaN substrates. XRD analysis demonstrates that the Mn-doped substrates' dislocation density is higher. The DC characteristics of the Mn-doped device are superior to those of the Fe-doped devices. Despite being lower, its advantages can be seen in variable-temperature measurements. At high temperatures, its current decay is slower, and its substrate transmission line loss is lower, lowering its leakage current, which in turn affects its high-frequency characteristics. Because of the good trend and high-frequency power conversion efficiency, the Mn-doped substrate can have more stable characteristics at variable temperatures and help improve high-frequency characteristics.

REFERENCES

[1] Y. Zhou, D. Wang, C. Ahyi, C.-C. Tin, J. Williams, M. Park, et al., "High breakdown voltage Schottky rectifier fabricated on bulk n-GaN substrate," Solid-State Electronics, vol. 50, pp. 1744-1747, Nov 2006.

[2] "AlGaN/GaN on SiC Device without a GaN Buffer Layer: Electrical and Noise Characteristics," Multdisciplinary Digital Publishing Institute, Micromachines,11(12),1131, Dec 2020.

[3] D.-Y. Chen, " Microwave Performance of 'Buffer-Free' GaN-on-SiC High Electron Mobility Transistors," IEEE Electron Device Letters, vol. 41, pp. 828-831, Apr 2020.

[4] A. F. Wilson, A. Wakejima, and T. Egawa, "Influence of GaN stress on threshold voltage shift in AlGaN/GaN high-electron-mobility transistors on Si under off-state electrical bias," Applied physics express, vol. 6, no. 8, p. 086504, 2013.

[5] V. L. Ene et al., "Study of Edge and Screw Dislocation Density in GaN/Al_2O_3 Heterostructure," Materials, vol. 12, no. 24, p. 4205, 2019.

[6] Z. Tang, S. Huang, X. Tang, B. Li, and K. J. Chen, "Influence of AlN passivation on dynamic ON-resistance and electric field distribution in high-voltage AlGaN/GaN-on-Si HEMTs," IEEE Transactions on Electron Devices, vol. 61, no. 8, pp. 2785-2792, 2014.

[7] J. Shen et al., " High-mobility n−-GaN drift layer grown on Si substrates," Applied Physics Letters, vol. 118, no. 22, p. 222106, 2021.

[8] M. Iwinska et al., "Iron and manganese as dopants used in the crystallization of highly resistive HVPE-GaN on native seeds," Japanese Journal of Applied Physics, vol. 58, no. SC, p. SC1047, 2019.

[9] A. Wolos, M. Palczewska, M. Zajac, J. Gosk, M. Kaminska, A. Twardowski, M. Bockowski, I. Grzegory, and S. Porowski , "Optical and magnetic properties of Mn in bulk GaN," Phys. Rev. B 69, 115210 – Published 19 March 2004

,"